

Miscible viscous fingering induced by a simple $A+B\rightarrow C$ chemical reaction

T. Gérard and A. De Wit

Nonlinear Physical Chemistry Unit and Centre for Nonlinear Phenomena and Complex Systems, CP 231, Faculté des Sciences, Campus Plaine, Université Libre de Bruxelles (ULB), 1050 Brussels, Belgium

(Received 1 August 2008; published 27 January 2009)

Viscous fingering (VF) is a hydrodynamical instability that occurs in porous media when a less viscous fluid displaces a more viscous one. We investigate here numerically how such an instability can be triggered by a simple $A+B\rightarrow C$ reaction when a solution of one reactant is displacing linearly a miscible solution of another reactant of same viscosity producing a more viscous product C at the interface. The properties of the fingering pattern observed in the zone where the less viscous reactant pushes more viscous products are studied as a function of the relevant parameters of the problem. These are the Damköhler number, the viscosity contrast between reactants and product, the ratio of initial concentrations of A and B , and the diffusion coefficients of each species. Our study shows that the fingering pattern can in some cases be different whether A displaces B or vice versa, enlightening recent experimental observations of such asymmetries in micellar systems. In particular, we show that in this asymmetric case, VF is more intense when the invading chemical solution is either the less concentrated one for equal diffusivities or when it contains the slower diffusing reactant for fixed equimolar initial concentrations.

DOI: 10.1103/PhysRevE.79.016308

PACS number(s): 47.70.Fw, 47.56.+r, 47.20.Gv

I. INTRODUCTION

Fingering patterns occurring when a less viscous fluid displaces a more viscous one in a porous medium have long been studied in nonreactive systems [1–3]. In reactive systems, the fingering dynamics depends whether the chemical species are passively advected by the flow or whether they are actively influencing it. In the case of passive scalars, the fingering properties of the interface remain those of nonreactive fluids even though the flow has clearly an influence on the spatiotemporal distribution of the chemicals [4–7]. The situation of interest here is the other case where the chemical reaction plays an active role on the viscous fingering (VF) instability.

The dynamics of chemically driven VF depends then whether the two fluids at hand are miscible or not and whether the chemical reaction modifies the physical properties of the porous matrix or not. It has been known for quite a long time in the literature focusing on “reactive infiltration instabilities” that viscous fingering patterns can be induced by a dissolution reaction affecting the porosity of the porous medium [8–10]. More recently, the reverse case of a reaction involving precipitation decreasing mobility inside a Hele-Shaw cell [11] or adsorption phenomena upon the porous matrix [12] has also been shown to affect fingering. For practical purposes, it is, however, interesting to understand active influence of chemistry on VF without affecting the properties of the porous medium itself. This can be done thanks to chemical reactions changing the surface tension of immiscible interfaces or the viscosity of the fluids.

In this regard, the influence of a simple acid-base neutralization reaction on the Saffman-Taylor instability has been studied experimentally between two immiscible fluids showing that the reaction changes the surface tension at the interface, which in turn modifies the viscous fingering pattern [13–15]. In the case of miscible viscous fingering, numerical work has analyzed the fingering pattern when viscosity is

modified with concentration across an autocatalytic bistable traveling front [10,16–18]. Besides frontal polymerization fronts [19], no clear evidence of viscosity changes across autocatalytic fronts has been obtained experimentally as these redox reactions are more prone to yield density differences in the course of reaction [20] rather than viscosity jumps. As suggested in [21], simple chemical reactions of the type



are more prone to provide viscosity differences needed to trigger VF phenomena. In this regard Nagatsu *et al.* [22] have recently succeeded in actively modifying miscible VF properties by such a bimolecular reaction. The chemical reaction can either decrease or increase the viscosity at the miscible interface, modifying in this way the properties of the fingering pattern. In this case, however, the reaction is modifying an already existing fingering instability as the reactant injected into the other one is genuinely chosen to be less viscous.

In parallel, Podgorski *et al.* have also performed recently experiments on VF fully triggered by a simple $A+B\rightarrow C$ reaction at the interface between two solutions of A and B of same viscosity [23]. In this system, the two fluids are aqueous solutions of different reactants that form a viscoelastic micellar product upon contact and reaction [24]. As the two reactant solutions have the same viscosity, no VF can be observed in the absence of reaction and the VF patterns result thus truly from the reaction at the miscible “interface” where the two reactants meet, triggering a hydrodynamic instability. An interesting result of this study was the observation that the VF pattern is different depending whether reactant A is injected into reactant B or vice versa. The authors conjectured that this could be due to a difference in diffusion coefficients of the various chemical species.

In this context, it is our objective to enlighten to what extent a simple $A+B \rightarrow C$ reaction is able to trigger VF when two miscible solutions of reactants A and B of same viscosity are put into contact. We further analyze to what extent the properties of the VF pattern depend on the values of the parameters of the problem. To do so, we numerically study a porous system in which one reactant is linearly injected into a miscible solution of the other reactant of same viscosity, producing at the interface a more viscous product. We analyze the properties of the resulting VF pattern as a function of the Damköhler number of the problem, of the viscosity ratio between product and reactants, of the diffusion coefficients of the species, and of the ratio of initial concentrations of A and B . We show that the VF pattern is different whether A displaces B or vice versa only when the underlying reaction-diffusion concentration profiles are not symmetric in time with regard to the initial position of the interface. This happens when the reactants A and B have different diffusion coefficient or are put in contact with different initial concentrations.

The paper is organized as follows: In Sec. II, we introduce the model describing VF induced by a simple $A+B \rightarrow C$ reaction, recall the properties of the underlying reaction-diffusion system, and explain our numerical procedure. In Sec. III, the results of the nonlinear simulations with a discussion of the influence of the various parameters of the system on the dynamics are presented before conclusions are drawn in Sec. IV where suggestions of experiments to test our predictions are given.

II. MODEL SYSTEM

A. Basic equations

We consider a homogeneous two-dimensional porous medium of length L_x and width L_y with constant permeability κ . Alternatively, this system also describes dynamics in a Hele-Shaw cell (two glass plates separated by a thin gap width l) when $l \ll L_x, L_y$ in which case $\kappa = l^2/12$. In this system, a solution of reactant B with initial concentration b_0 is sandwiched between miscible solutions of another reactant A with initial concentration a_0 (see Fig. 2). The two solutions are both considered diluted and to have the same viscosity μ_0 . A simple chemical reaction



takes place at the interface where A and B meet producing a product C more viscous than the reactants. We consider here that $b_0 \geq a_0$ so that the final concentration of the product if the reaction would be conducted in a stirred reactor is $c_0 = a_0$. We seek to understand how the interface between the reactants and the product can be destabilized by viscosity differences when the reactive solutions are displaced linearly in the porous medium or Hele-Shaw cell at constant injection speed U . Indeed, in that case, viscous fingering will occur at the interface where the less viscous reactant pushes the more viscous product. As the system is considered neutrally buoyant, the dynamics can be described by the following system of reaction-diffusion-convection (RDC) equations:

$$\nabla \cdot \mathbf{u} = 0, \quad (3)$$

$$\nabla p = -\frac{\mu(c)}{\kappa} \mathbf{u}, \quad (4)$$

$$\frac{\partial a}{\partial t} + \mathbf{u} \cdot \nabla a = D_A \nabla^2 a - kab, \quad (5)$$

$$\frac{\partial b}{\partial t} + \mathbf{u} \cdot \nabla b = D_B \nabla^2 b - kab, \quad (6)$$

$$\frac{\partial c}{\partial t} + \mathbf{u} \cdot \nabla c = D_C \nabla^2 c + kab, \quad (7)$$

where a , b , and c denote, respectively, the concentrations of the two reactants A and B and of the product C , k is the kinetic constant, p is the pressure, and $\mathbf{u} = (u, v)$ is the two-dimensional velocity field, while $D_{A,B,C}$ are the diffusion coefficients of the species A , B , and C , respectively. Equation (4) is Darcy's law relating the velocity field \mathbf{u} to the gradient of pressure ∇p , with κ the permeability. The viscosity $\mu = \mu(c)$ of the fluid is supposed to be a function of the local concentration $c(x, y, t)$ of the product only, the viscosity of the reactant solution when $c=0$ being μ_0 , the viscosity of the solvent. We assume furthermore that the viscosity of the fluid varies exponentially with the concentration c so that

$$\mu(c) = \mu_0 e^{R(c/c_0)}, \quad (8)$$

where R is the log-mobility ratio defined as

$$R = \ln \left[\frac{\mu(c = c_0)}{\mu_0} \right]. \quad (9)$$

The parameter R is thus a measure of the ratio between the viscosity of the final product solution (where c is in concentration $c_0 = a_0$) and that of the reactant solutions A and B where $\mu_0 = \mu(c=0)$. If the product solution has the same viscosity μ_0 than the reactants, the log-mobility ratio $R=0$ and no VF takes place. We recover in that case the pure $A+B \rightarrow C$ reaction-diffusion system, which has been the subject of numerous studies [25–28]. If $R > 0$, then the chemical reaction produces a more viscous product C at the interface between the less viscous reactants. Depending whether A is injected into B or vice versa VF will develop at the interface where A invades C or where B displaces C , respectively—i.e., at the interface where the less viscous reactant pushes the more viscous product. The choice of an initial configuration of B sandwiched between A (Fig. 2) allows one to follow both cases at the same time.

Since the solutions are injected with a constant velocity U , we switch to a reference frame moving with U taking $x' = x - Ut$ and $\mathbf{u}' = \mathbf{u} - U\mathbf{e}_x$ where \mathbf{e}_x is the unit vector along direction x . The field equations become [2]

$$\nabla' \cdot \mathbf{u}' = 0, \quad (10)$$

$$\nabla' p = -\frac{\mu(c)}{\kappa} (\mathbf{u}' + U\mathbf{e}_x), \quad (11)$$

$$\frac{\partial a}{\partial t} + \mathbf{u}' \cdot \nabla' a = D_A \nabla'^2 a - kab, \quad (12)$$

$$\frac{\partial b}{\partial t} + \mathbf{u}' \cdot \nabla' b = D_B \nabla'^2 b - kab, \quad (13)$$

$$\frac{\partial c}{\partial t} + \mathbf{u}' \cdot \nabla' c = D_C \nabla'^2 c + kab. \quad (14)$$

We then nondimensionalize the equations by the characteristic velocity U , hydrodynamical time $\tau_h = D_C/U^2$, length $L_h = D_C/U$, and concentration a_0 . The dimensionless concentrations $a' = a/a_0$ and $c' = c/a_0$ vary thus between 0 and 1, while $b' = b/a_0$ varies between 0 and ϕ where $\phi = b_0/a_0$. Viscosity is normalized by μ_0 and pressure as $p' = \frac{p\kappa}{\mu_0 D_C}$. We further introduce the ratios between diffusion coefficients of the reactants and the products, $\delta_A = D_A/D_C$ and $\delta_B = D_B/D_C$, as well as the dimensionless Damköhler number

$$D_a = \frac{D_C k a_0}{U^2}, \quad (15)$$

which corresponds to the ratio between the hydrodynamic time τ_h and the chemical time $\tau_c = 1/ka_0$. After dropping the primes, we obtain the following dimensionless equations in the moving frame:

$$\nabla \cdot \mathbf{u} = 0, \quad (16)$$

$$\nabla p = -\mu(c)(\mathbf{u} + \mathbf{e}_x), \quad (17)$$

$$\frac{\partial a}{\partial t} + \mathbf{u} \cdot \nabla a = \delta_A \nabla^2 a - D_a ab, \quad (18)$$

$$\frac{\partial b}{\partial t} + \mathbf{u} \cdot \nabla b = \delta_B \nabla^2 b - D_a ab, \quad (19)$$

$$\frac{\partial c}{\partial t} + \mathbf{u} \cdot \nabla c = \nabla^2 c + D_a ab. \quad (20)$$

Taking the curl of Eq. (17) and introducing the stream function $\psi(x, y)$ defined such that $u = \partial\psi/\partial y$ and $v = -\partial\psi/\partial x$, we have

$$\nabla^2 \psi = R(\psi_x c_x + \psi_y c_y + c_y), \quad (21)$$

$$a_t + a_x \psi_y - a_y \psi_x = \delta_A \nabla^2 a - D_a ab, \quad (22)$$

$$b_t + b_x \psi_y - b_y \psi_x = \delta_B \nabla^2 b - D_a ab, \quad (23)$$

$$c_t + c_x \psi_y - c_y \psi_x = \nabla^2 c + D_a ab. \quad (24)$$

Note that in absence of any reaction ($D_a = 0$), Eqs. (21) and (24) correspond to the classical VF model [2,3] of a less viscous solution with $c=0$ displacing a more viscous one where $c=c_0$ when the viscosity varies with c . In our dimensionless scales, the dimensionless domain width and length are Peclet numbers

$$Pe = UL_y/D_C, \quad (25)$$

$$Pe' = UL_x/D_C, \quad (26)$$

where Pe determines the number of fingers present across the domain, while Pe' controls the maximum time of the simulations.

B. Reaction-diffusion $A+B \rightarrow C$ system

The reaction-diffusion (RD) properties of a simple $A+B \rightarrow C$ system where the reactants A and B , with initial concentration ratio $\phi = b_0/a_0$, are put in contact at $t=0$ at a location $x=0$ have been studied in numerous articles since the pioneering work of Gálfi and Rácz [25]. When A and B meet by diffusion, they react producing C at the miscible interface. In the course of time, A and B are consumed by the reaction and hence the reaction rate decreases while more and more C is produced. At long times—i.e., in the diffusion-limited regime—it has been shown [25] that the width of the front scales in time like $\sim t^{1/6}$ and the maximum reaction rate [defined here as the maximum of the reaction rate curve $\mathcal{R}(x) = D_a a(x)b(x)$] goes like $\sim t^{-2/3}$.

The reaction front position defined as the location where \mathcal{R} is maximum stays at $x=0$ if A and B have the same diffusion coefficient and are initially present in the same concentration ($\phi=1$) as shown in Fig. 1(a). If this is not the case (explicitly if $a_0^2 D_A \neq b_0^2 D_B$) [25–28], the diffusive flux of A differs from that of B towards the reaction zone and the front moves towards the region which has the smallest diffusive flux. As an example, for $\delta_A = \delta_B$, it is the more concentrated solution that invades the other one [Fig. 1(b)], while when $\phi=1$, the front invades the reactant of lowest diffusion coefficient [Fig. 1(c)]. Depending on the parameters, the RD concentration profiles of reactants A and B and of the product C can thus be either symmetric or asymmetric with regard to the initial position of the front. From these profiles, it can be anticipated that, in the symmetric case, the VF pattern will be the same whether A displaces B or vice versa because the gradients of concentration (and hence of viscosity) between A and C will be the same as between B and C [case of Fig. 1(a)]. On the contrary, VF is expected to be different in the asymmetric case—i.e., as soon as $a_0^2 D_A \neq b_0^2 D_B$. This is fully borne out by numerical simulations as we will show it in the remainder of the paper.

C. Numerical procedure

To numerically integrate Eqs. (21)–(24) we follow the numerical scheme described in detail in Ref. [3] and adapted to take the chemical reaction into account [10,16]. It consists of a pseudospectral method using periodic boundary conditions in both longitudinal and transverse directions. As initial condition we consider a constant linear velocity U corresponding to a zero velocity relative to the translating frame—i.e., $\psi=0$ everywhere. For the concentrations, we start from the situation depicted in Fig. 2; i.e., we take two step fronts between the reactive solutions of A and B with random noise added in the fronts to trigger the instability on reasonable computing time. It is known that the nonlinear fingering pattern will be different for each different realization of the noise for a fixed given amplitude [29]. Hence, to compare

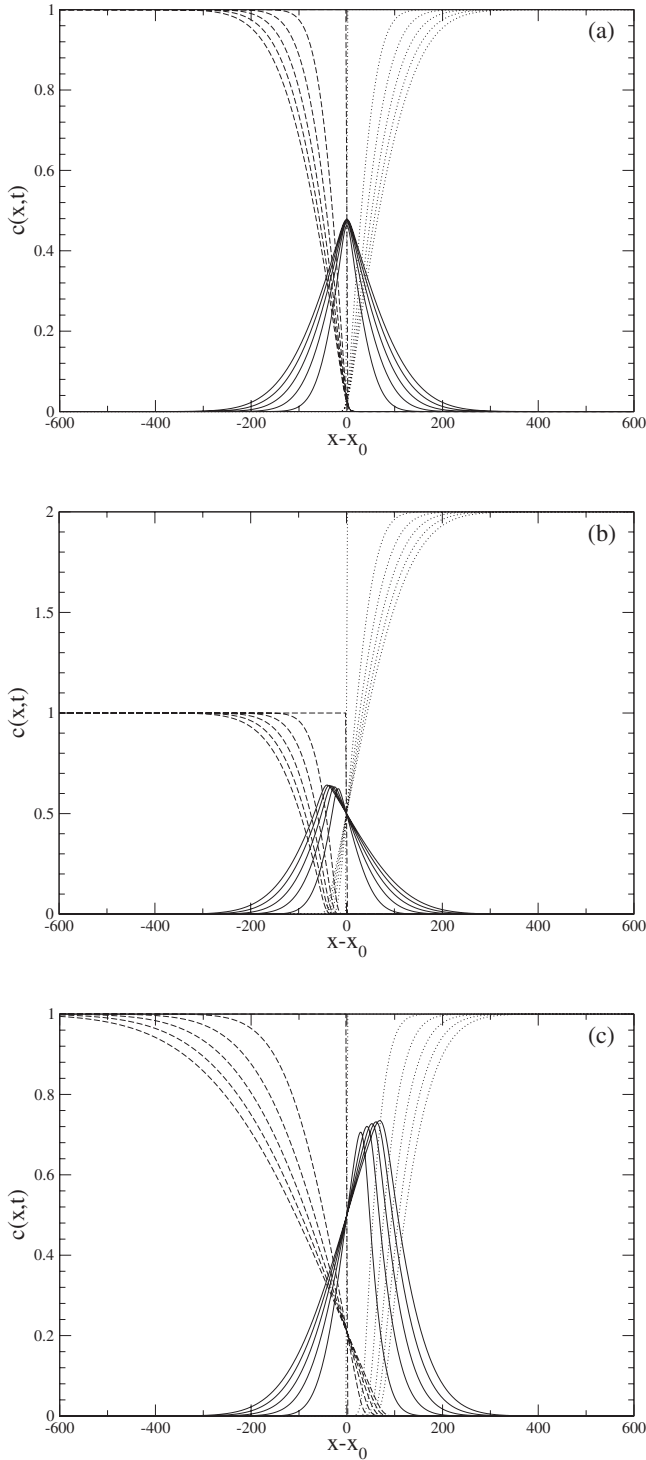


FIG. 1. One-dimensional RD concentration profiles of A (dashed lines), B (dotted lines), and C (solid lines) for $D_a=1$, $\delta_B=1$ and, respectively, (a) $\delta_A=1$, $\phi=1$, (b) $\delta_A=1$, $\phi=2$, and (c) $\delta_A=5$, $\phi=1$ at times $t=0, 1000, 2000, 3000, 4000$, and 5000 . x_0 is the position of the front at $t=0$.

the dynamics of the interface where A is injected into B with the reverse case where B pushes A, we seed the fronts with a noise triggering the same pattern. To do so we take as initial condition $c=0$ and $\psi=0$ everywhere with

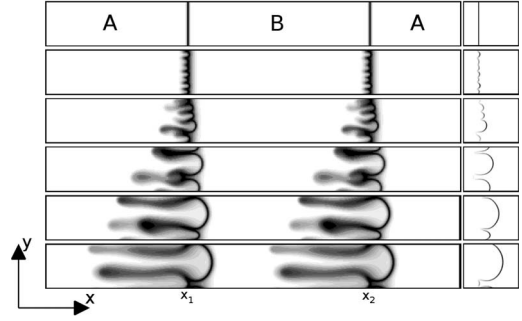


FIG. 2. Concentration of the product C (left) and reaction rate \mathcal{R} (right) for $R=3$, $D_a=1$, $\phi=1$, and $\delta_A=\delta_B=1$ at times $t=100, 1000, 2000, 3000, 4000$, and 5000 from top to bottom.

$$(a,b) = \begin{cases} (1,0) & \text{for } 0 < x < x_1, \\ (0.5 + \xi r, (0.5 - \xi r)\phi) & \text{at } x = x_1, \\ (0, \phi) & \text{for } x_1 < x < x_2, \\ (0.5 - \xi r, (0.5 + \xi r)\phi) & \text{at } x = x_2, \\ (1,0) & \text{for } x_2 < x < \text{Pe}', \end{cases} \quad (27)$$

with r a random number between 0 and 1 and ξ an amplitude of value 10^{-2} . x_1 and x_2 are the initial positions of the two interfaces of Fig. 2.

To validate our code, we have checked that, when $R=0$ and no fingering takes place, we recover the scalings of the stable RD profiles known in the literature [25–27]. The results of our simulations are displayed as density plots of the concentration fields with a gray scale ranging from black for $(a,b,c)=(1,\phi,1)$ to white when the concentrations are zero.

III. REACTIVE VISCOUS FINGERING DYNAMICS

A. Symmetric vs asymmetric nonlinear dynamics

Figure 2 presents a typical reactive VF dynamics for $R=3$ and $D_a=1$ in a system where B is sandwiched between A in the symmetric case where the reactants have the same diffusion coefficients ($\delta_A=\delta_B=1$) and are present in the same initial concentrations ($\phi=1$). In our reference frame moving with injection speed U , fingering develops around the fixed initial position of the interface where A and B meet. As the chemical reaction produces a more viscous product, the interface is unstable both where A pushes the product C and where B displaces C. As the RD concentration profiles are symmetric in this case around the locations x_1 and x_2 and for our choice of noise seeding the initial condition, the VF pattern is exactly the same on both interfaces. At onset, several fingers appear, which start to interact at later times. As in nonreactive VF, fingers elongate more in the region of the invading less viscous solution, more advanced fingers shield their neighbors, and coarsening is observed in the course of time due to merging phenomena [3,31]. Figure 2 also displays the reaction rate

$$\mathcal{R}(x,y,t) = D_a a(x,y,t) b(x,y,t). \quad (28)$$

It can be seen that reaction occurs only where A and B meet and that, even if fingers of the product C are developing

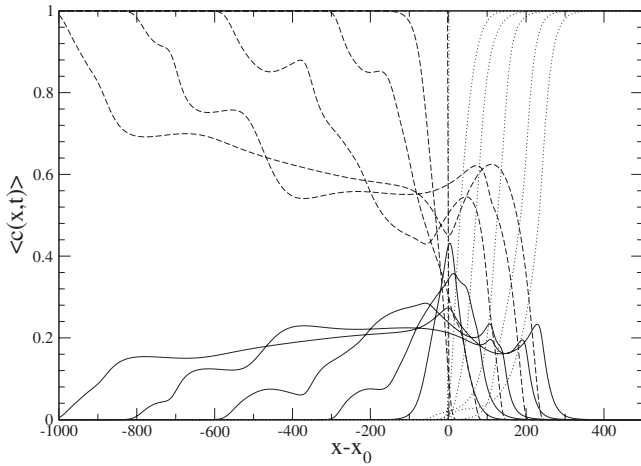


FIG. 3. Transversely averaged concentration profiles of *A* (dashed lines), *B* (dotted lines), and *C* (solid lines) for the simulations of Fig. 2 at times $t=0, 1000, 2000, 3000, 4000,$ and 5000 with x_0 being the position of the front at $t=0$.

more in the displacing reactant—i.e., to the left here—the reaction zone travels on average more to the right. This is due to the fact that convection entrains fresh invading reactant more rapidly to the right in the middle of fingers than diffusion transports the invaded reactant to the left. Even if the fingering zone extends thus on a large distance, the reaction rate distribution remains very localized around the right part of the extended product *C* distribution.

Let us note that all variations of parameters that maintain the symmetry of the one-dimensional (1D) RD profiles as seen in Fig. 1(a) will feature the same VF pattern at x_1 and x_2 ; i.e., fingering properties will remain the same whether *A* invades *B* or vice versa. This is typically the case if the log-mobility ratio R or the Damköhler number D_a are varied. Indeed, a change in R does not affect the RD system, but affects only the intensity of fingering, which increases with R . If D_a is modified, the amplitude of the 1D RD concentration curves is modified in the scaling used here, but not their symmetry with regard to $x=0$ as D_a rescales only the time of the reaction process with regard to the convective time. Furthermore, the diffusion coefficient of *C* is also unimportant for the symmetry (see Fig. 8) as the absolute value of D_C can affect the intensity of fingering by modifying the intensity of δ_A and δ_B , but not the symmetric or asymmetric character of the RD profiles with regard to $x=0$, which depends solely on $D_A, D_B, a_0,$ and b_0 .

We understand thus that asymmetric VF between the left and right interfaces where *A* displaces *B* and vice versa, respectively, can be obtained only if $\delta_A \neq \delta_B$ or $\phi \neq 1$.

B. Quantitative analysis

The properties of this reaction-driven VF can usefully been examined by computing several quantities. First of all, the two-dimensional concentration profiles $c(x,y,t)$ can be averaged along the transverse coordinate y to yield the one-dimensional transversely averaged concentration profile

$$\langle c(x,t) \rangle = \frac{1}{\text{Pe}} \int_0^{\text{Pe}} c(x,y,t) dy. \tag{29}$$

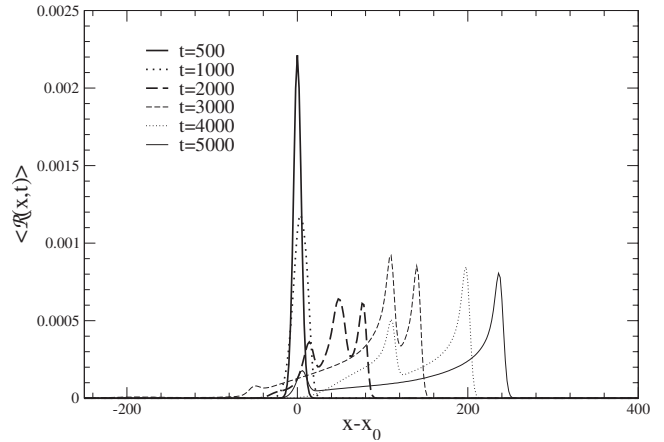


FIG. 4. Transversely averaged profiles of the reaction rate \mathcal{R} for the simulations of Fig. 2.

For $R=0$, these profiles are equivalent to the 1D RD profiles shown in Fig. 1 as no VF takes place and the concentration fields remain homogeneous in the transverse direction. In the presence of VF, these transversely averaged profiles feature bumps characteristics of the presence of fingers (see Fig. 3) and have their center of gravity that is displaced to the back as observed in nonreactive fingering of finite-size samples [29,30]. Such transversely averaged profiles can also be obtained for the reaction rate distribution (28) to obtain 1D curves $\langle \mathcal{R}(x,t) \rangle$ as shown in Fig. 4. From the transversely averaged concentration profiles, one can next compute the length of the fingering zone defined here as the length of the zone where $\langle c(x,t) \rangle$ is above 0.01. In the absence of convection, the fingering length grows as \sqrt{t} characteristic of a diffusive process, while it grows quicker in the presence of convection. This can be seen in Fig. 5 that displays the temporal evolution of the mixing length for various values of parameters. The default values are $R=3, D_a=1, \delta_A=\delta_B=1,$ and $\phi=1$. To perform a parametric study, one parameter at a time is then changed to the value in the inset of the figure.

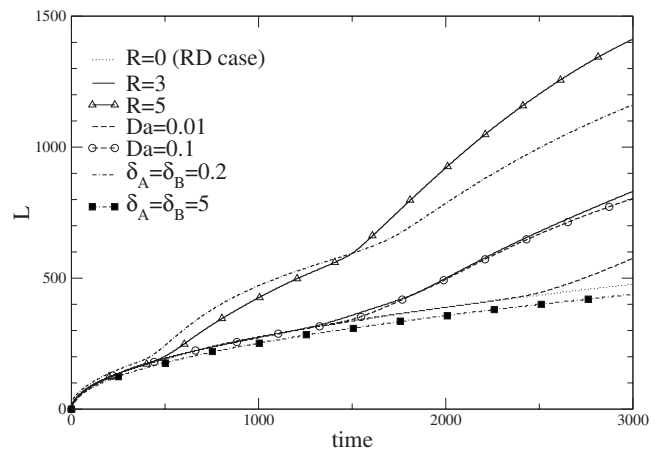


FIG. 5. Temporal evolution of the fingering length for different parameters. The default values used to obtain the solid curve are $R=3, D_a=1, \delta_A=\delta_B=1,$ and $\phi=1$. The other curves are obtained by changing one parameter at a time to the value given in the inset.

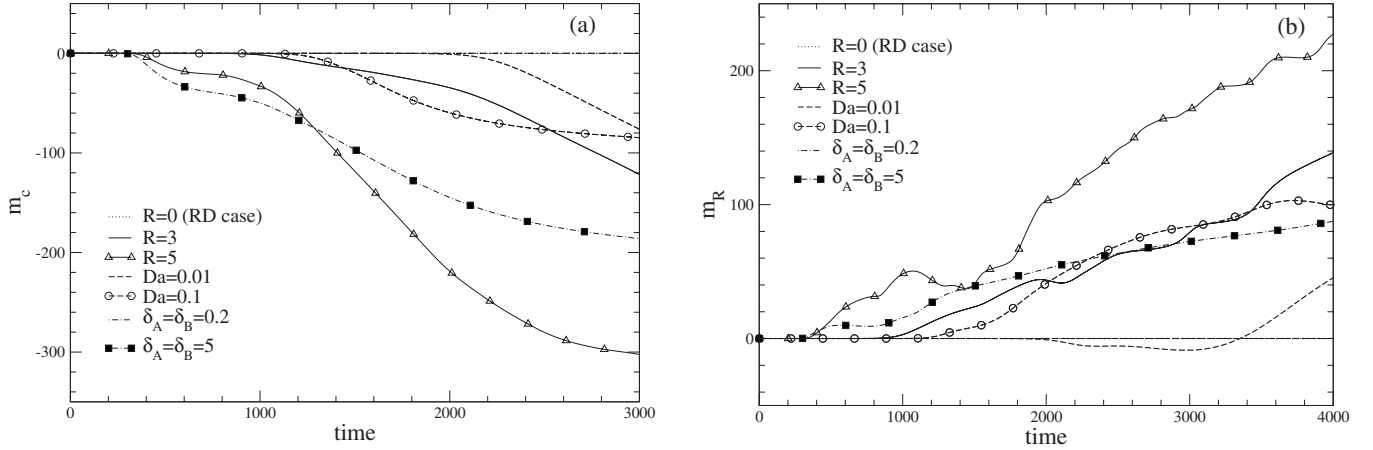


FIG. 6. Temporal evolution of (a) m_c the location of the center of mass (first moment) of $\langle c(x,t) \rangle$ and (b) m_R the first moment of the reaction rate $\langle \mathcal{R}(x,t) \rangle$ distribution for different values of the parameters along the same convention as in Fig. 5.

The center of mass m_c of this 1D product concentration distribution can also be computed as the first moment of the $\langle c(x,t) \rangle$ curves [29] [Fig. 6(a)]. It is observed to move towards the back—i.e., towards negative values of $x-x_0$ (x_0 being the initial position of the interface—i.e., x_1 or x_2)—in agreement with what is observed visually in the transversely averaged profiles of Fig. 3. We also follow in time the first moment m_R of the 1D transversely averaged production rate $\langle \mathcal{R}(x,t) \rangle$ [Fig. 6(b)]. Contrary to m_c , we see here that m_R is moving in time to the right (positive $x-x_0$) where convection is pushing the reactants.

Eventually, in reactive systems, it is interesting to have insight into the influence of convection on the yield of the reaction. To do so, we compute the total amount c_{tot} of product C [Fig. 7(a)] or the total reaction rate \mathcal{R}_{tot} [Fig. 7(b)] obtained in the course of time by integrating along both directions, respectively $c(x,y,t)$ or $\mathcal{R}(x,y,t)$, on the domain of interest—i.e., on the left or right half, respectively, of the system. Concerning the total reaction rate \mathcal{R}_{tot} , we note that, for RD systems (dotted line, $R=0$), the reaction rate is strong at the start and decreases next in time when the system enters a diffusion-limited dynamics [25]. For RDC systems, on the contrary, the onset behavior is identical because it takes time to the instability to appear, but once convection is active, \mathcal{R}_{tot} grows again. This is due to the fact that, at the unstable side, convection brings continuously fresh reactants to the front and keeps thus feeding the reactive process. Because the reaction rate is larger with convection than without it, the total amount of product is also increasing more in systems which finger as seen in Fig. 7.

On the basis of the various quantities introduced here, let us now examine the influence of the various parameters of the problem on the reactive VF dynamics.

IV. PARAMETRIC STUDY

This problem depends on two different types of parameters: some parameters affect all the species in the same way like R , D_a , and δ_C (used to nondimensionalize diffusion coefficients). Their variation affects therefore equally fingering

on both left and right interfaces, and they keep the dynamics symmetric; i.e., the fingering should be the same on average whether A pushes B or vice versa. Other parameters affect only one species at the time like ϕ , δ_A , and δ_B . Their variation induces therefore an asymmetry in the underlying RD concentration profiles of the base state and hence lead to

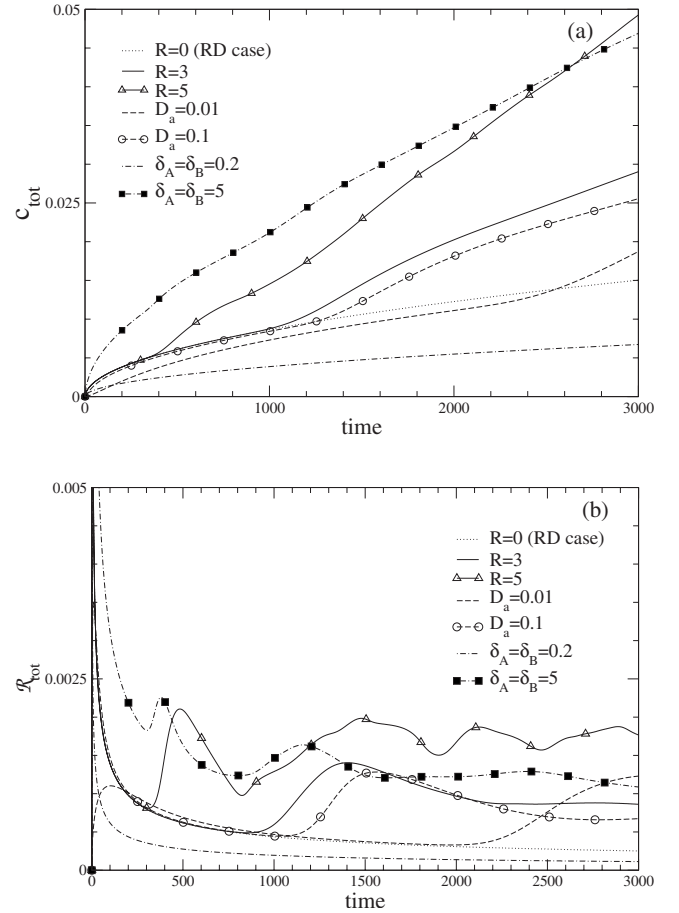


FIG. 7. Temporal evolution of (a) the total product concentration c_{tot} and (b) the total reaction rate \mathcal{R}_{tot} for different values of the parameters along the same convention as in Fig. 5.

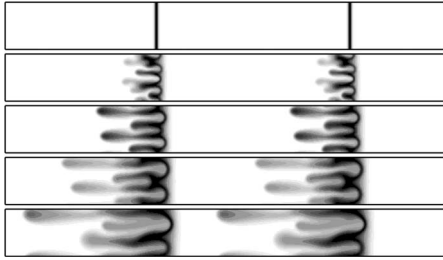


FIG. 8. Concentration of the product C for for the same parameters as in Fig. 2 except $\delta_A = \delta_B = 5$ at times $t = 100, 1000, 2000, 3000$ and 4000 .

asymmetries in the fingering response whether A pushes B or vice versa. Let us therefore examine their influence separately.

A. Symmetric fingering

If the viscosity ratio R is increased, the system is more unstable, VF more vigorous, and fingers more elongated just as in nonreactive systems. This has for effect to increase the width of the zone where the product is present and hence to increase the fingering length. This influence of the change in R can be appreciated in Figs. 5–7 by comparing the curves for fixed $D_a = 1, \delta_A = \delta_B = 1,$ and $\phi = 1,$ but increasing R . In parallel, the center of mass of the product distribution is further shifted to the left when R increases [Fig. 6(a)], while the first moment of the reaction rate distribution is further shifted to the right [Fig. 6(b)]. From the point of view of the chemist, increased convection has a beneficial effect as c_{tot} , the total amount of C produced in time, as well as the total production rate \mathcal{R}_{tot} are all increasing functions of R (Fig. 7).

If the Damköhler number D_a is decreased, it means that the reaction time is increased with regard to the hydrodynamic time; i.e., fewer reaction steps and thus less C is produced per unit of dimensionless time which does not favor the VF instability. This can be seen in Figs. 5–7 by comparing curves for fixed $R = 3, \delta_A = \delta_B = 1,$ and $\phi = 1$ and $D_a = 0.001, 0.1,$ and $1,$ respectively. A decrease of D_a decreases the fingering length (Fig. 5), c_{tot} , and \mathcal{R}_{tot} (Fig. 7), while the center of mass of the product distribution is less shifted to the left [Fig. 6(a)] and the instability starts later.

Eventually we can also vary the diffusion coefficient of the product C , which is done here in our dimensionless units

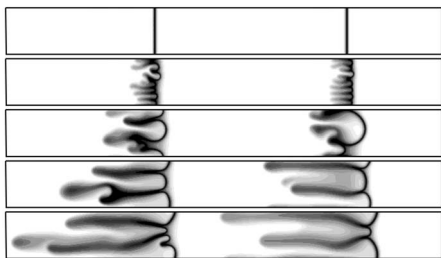


FIG. 9. Concentration of the product C for the same parameters as in Fig. 2 except $\phi = 2$ at times $t = 100, 1000, 2000, 3000,$ and 4000 .

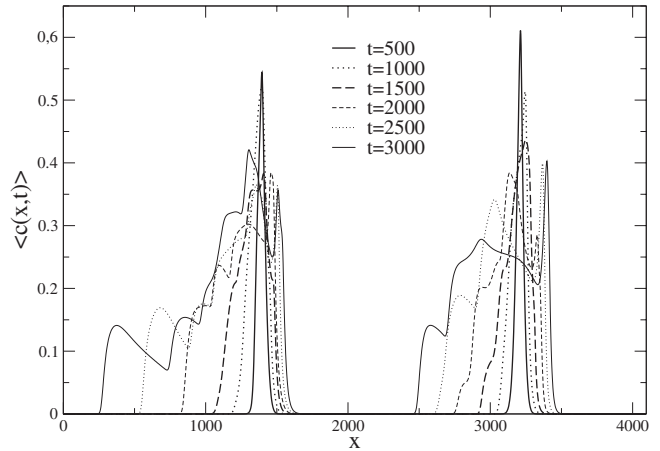


FIG. 10. Transversely averaged concentration profiles $\langle c(x,t) \rangle$ for the simulation of Fig. 9.

by changing simultaneously δ_A and δ_B in the same way. If $\delta_A = \delta_B$ is increased (i.e., D_C is decreased), the viscous products escape slower the reaction zone, viscosity gradients are sharper, and the front is more unstable. To see this, compare Figs. 2 and 8, which shows that fingers appear quicker and extend farther away at a given later time for $\delta_A = \delta_B = 5$ than for $\delta_A = \delta_B = 1$. On the contrary, if C is the fastest diffusing species, $\delta_A = \delta_B < 1$ and the system is more stable as the viscous product C diffuses quicker out of the interface and the viscosity gradients are hence weaker. This is confirmed with the fact that the fingering length (Fig. 5), c_{tot} , and \mathcal{R}_{tot} (Fig. 7) are all increasing functions when $\delta_A = \delta_B$ are increased as can be seen comparing the full curve for $R = 3, D_a = 1, \phi = 1,$ and $\delta_A = \delta_B = 1$ with those for which $\delta_A = \delta_B = 0.2$ or $5,$ respectively.

B. Asymmetric fingering

Let us now examine the difference in VF of the left interface initially located at x_1 where A displaces B with the right

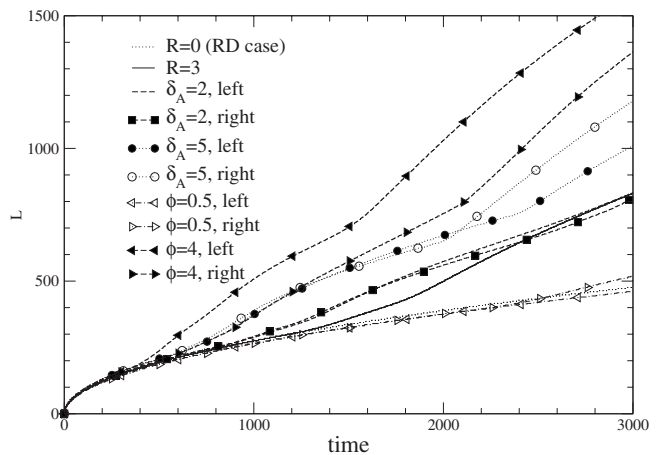


FIG. 11. Temporal evolution of the fingering length for different values of parameters following the convention of Fig. 5. The solid curve noted as “ $R = 3$ ” in the inset corresponds to the values of parameters $R = 3, D_a = 1, \delta_A = \delta_B = 1,$ and $\phi = 1$. The extent of L in time is different on the left and right interfaces located at x_1 and $x_2,$ respectively, when $\phi \neq 1$ or $\delta_A \neq \delta_B$.

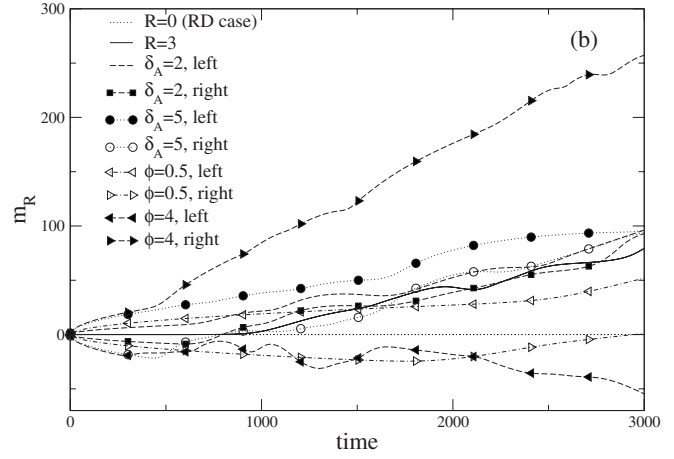
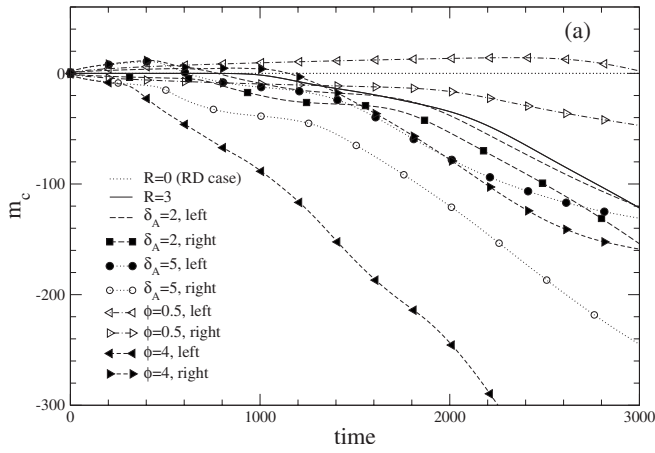


FIG. 12. Temporal evolution of (a) m_c the location of the center of mass (first moment) of $\langle c(x,t) \rangle$ and (b) m_R the reaction rate $\langle \mathcal{R}(x,t) \rangle$ distribution for different values of the parameters along the same convention as in Fig. 5. These evolutions are different for the left and right interfaces if $\phi \neq 1$ or $\delta_A \neq \delta_B$.

one where B invades A around the initial location x_2 in the case where the underlying RD system is asymmetric—i.e., if $\phi \neq 1$ or $\delta_A \neq \delta_B$. Let us analyze these two cases successively.

1. Influence of the ratio of initial reactant concentrations ϕ

The results presented up to now were all obtained with $\phi=1$ (i.e., $a_0=b_0$) and gave identical fronts whether A invades B or vice versa. If now $\phi \neq 1$, it is observed that the VF patterns (Fig. 9) and the related transversally averaged concentration profiles (Fig. 10) are different whether A invades B or vice versa. As can be seen in the concentration profiles of the corresponding RD system [Fig. 1(b)], if $\phi=2$ like in Fig. 9, the RD front is displaced into the zone of reactant A in time because B is more concentrated and invades thus the rate-limiting chemical species A . As one reactant is more concentrated than the other one, a first consequence is that more products can be formed per unit of time because the reaction rate is directly proportional to the reactant concentrations—i.e., $\mathcal{R} \sim ab$. In presence of VF—i.e., if

$R > 0$ —this increase of product concentration per unit of time is destabilizing the system. This can be appreciated by comparing in Figs. 11–13 the solid curve obtained for $R=3$, $D_a=1$, $\delta_A=\delta_B=1$, and $\phi=1$ with the curves obtained for the same parameters except $\phi=0.5$ or 4 . The dynamics is then different whether the focus is on the left or right interface. It is seen that, when ϕ is increased, the corresponding fingering length increases (Fig. 11) and the center of mass of the product distribution is further displaced to the left (Fig. 12), while the total amount of C produced per unit of time increases (Fig. 13).

A second consequence of the asymmetry in the RD concentration profiles [Fig. 1(b)] is that the viscosity gradient at the interface located in x_1 (left) where A pushes C is sharper than the one on the interface at x_2 (right) where B displaces C . VF is thus more intense and extends further around x_1 than around x_2 . Note that, at early times before VF sets in, the RD dynamics is such that B invades A and hence, during the first 200 units of time, the locations of m_c and m_r invade symmetrically with a square-root dependence the reactant A (see Fig. 12). In particular, for the front initially located in x_2

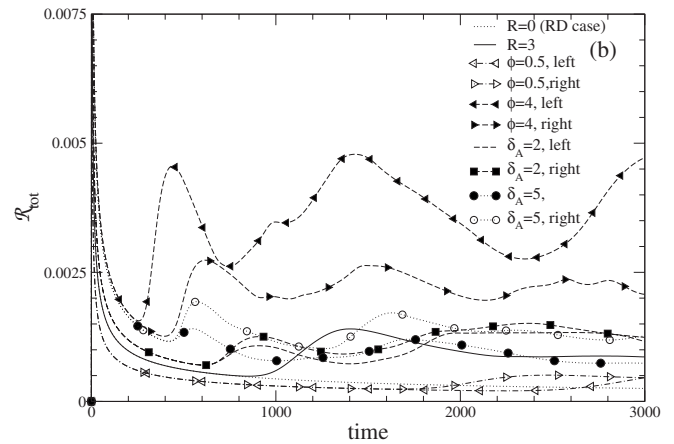
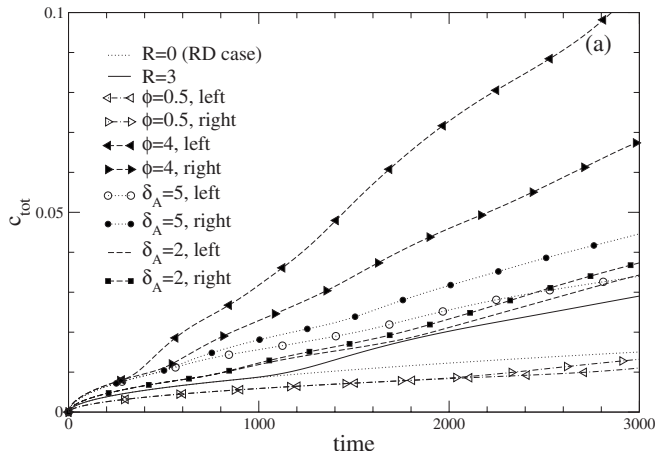


FIG. 13. Temporal evolution of (a) the total product concentration c_{tot} and (b) of the total reaction rate R_{tot} for different values of the parameters along the same convention as in Fig. 5. These evolutions are different for the left and right interfaces if $\phi \neq 1$ or $\delta_A \neq \delta_B$.

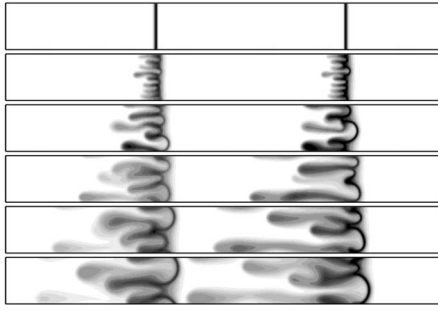


FIG. 14. Concentration of the product C for the same parameters as in Fig. 1 except $\delta_A=5$ at times $t=100, 1000, 2000, 3000, 4000,$ and 5000 .

(right), m_c travels first towards positive x (B invades A to the right) before turning back towards negative x when VF takes over. When $\phi > 1$ such that the RD front moves towards A , the concentration gradient is sharper for A than for B and thus VF is more intensive on the front where A displaces the product C than where B fingers into C . The reverse is obtained for $\phi < 1$. We can therefore conclude that as soon as $\phi \neq 1$ for $\delta_A = \delta_B$, VF will be more intense in the situation where the less concentrated solution is injected into the more concentrated one.

2. Influence of different reactant diffusion coefficient

For $\phi=1$, but when reactants have different diffusion coefficients, the RD front does not remain stationary either, but the fastest diffusing species invades the other one [see Fig. 1(c)]. Similarly, the gradients of concentrations are not symmetric and the VF pattern is different whether A invades B or vice versa. If A diffuses faster ($\delta_A > \delta_B$), then the concentration profile of A is more spread out [see Fig. 1(c)] than the one of B . The gradient of A being therefore smaller, VF will be less efficient at the interface where A is injected into B than where B displaces A as is seen in Figs. 14 and 15. Consequently, the fingering length is larger (Fig. 11) and m_c

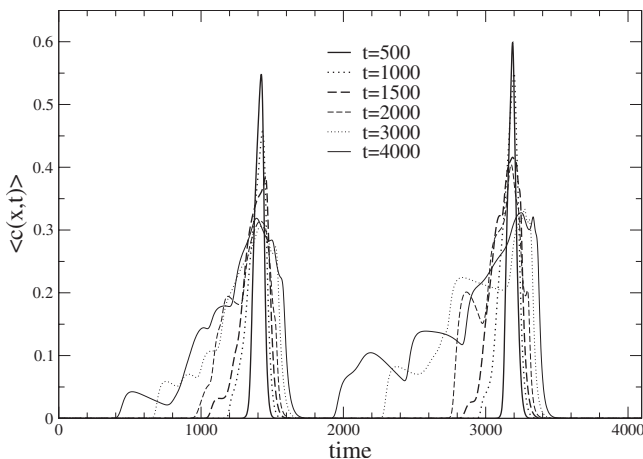


FIG. 15. Transversely averaged concentration profiles $\langle c(x,t) \rangle$ for the simulation of Fig. 14.

extends further away on the right interface located at x_2 than on the left one at x_1 (Fig. 13). These trends increase with δ_A at fixed δ_B . Similarly, c_{tot} is larger on the right interface than on the left one (Fig. 12). This reasoning leads us thus to understand that, for an equimolar initial concentration of both reactants ($\phi=1$), VF will be more intense when the slowest diffusing species is the one injected into the solution of the fastest diffusing species.

V. CONCLUSIONS

The objective of this paper has been to analyze by a theoretical approach how a chemical reaction can trigger VF in a system where the reactive displacing and displaced solutions both have the same viscosity but the chemical product produced at their interface is more viscous. To do so, we have numerically integrated Darcy's law in which the viscosity depends on the product concentration c coupled to RDC equations for the concentrations of the chemicals involved in a simple $A+B \rightarrow C$ reaction. We find that VF can be produced at the interface where a less viscous reactant pushes the more viscous product. This VF is symmetric whether A pushes B or vice versa if the underlying 1D RD concentration profiles are symmetric, which is the case if the ratio of initial reactant concentration $\phi=1$ and if the reactants diffuse at the same rate $\delta_A = \delta_B$. If this is not the case, then the VF pattern is different whether A invades B or vice versa. Between these two cases, the most unstable VF situation is then the one where the invading chemical solution is either less concentrated or contains the slowest diffusing species.

These results allow us to understand why VF patterns studied recently experimentally by Podgorsky *et al.* [23] are not symmetric depending whether one reactive solution is injected into the other one or vice versa when they used equally concentrated reactive solutions. The present results confirm that asymmetry is then due to the fact that the two reactants have different diffusion coefficients as conjectured by the authors. Let us note that the present work is only a first step toward a full description of such experiments where the viscoelastic properties of the product are important, while these effects are not taken into account here.

Our numerical results allow us also to suggest possible further experimental work. In particular, it would be nice to test the possibility that a simple change of the initial concentration of the reactants can drastically change the dynamics. Up to now, the experiments conducted in [23] have addressed only equally concentrated reactants (i.e., $\phi=1$). In this case, if the concentrations a_0 and b_0 are both increased equally to keep the ratio ϕ a constant, the system should be more unstable as more product C will then be produced. If one of the initial concentrations—say, a_0 —is kept constant, a change of b_0 will vary ϕ and will thus vary the VF properties along the lines described in Sec. IV B 1. In this regard, the present study suggests that the key parameter in understanding the dynamics is the parameter $\gamma = a_0^2 D_A / b_0^2 D_B = \delta_A / \phi^2 \delta_B$, which controls the direction of propagation of the underlying RD front. For a given experimental choice of reactant A and B and thus for a given ratio D_A/D_B , a change of initial

concentration ratio ϕ to bring γ from a value smaller than 1 to another value larger than 1 switches the direction of propagation of the RD front [25]. This should lead to visible changes in the VF pattern properties as this will modify the underlying RD gradients between the reactants and the product.

ACKNOWLEDGMENTS

We thank J. Azaiez and A. Belmonte for fruitful discussions. A.D. thanks Prodex, FRS-FNRS, and the Communauté française de Belgique (ARC Program) for financial support. T.G. benefits from support from FRIA.

-
- [1] G. M. Homsy, *Annu. Rev. Fluid Mech.* **19**, 271 (1987).
 [2] C. T. Tan and G. M. Homsy, *Phys. Fluids* **29**, 3549 (1986).
 [3] C. T. Tan and G. M. Homsy, *Phys. Fluids* **31**, 1330 (1988).
 [4] M. Jahoda and V. Hornof, *Powder Technol.* **110**, 253 (2000).
 [5] Y. Nagatsu and T. Ueda, *AIChE J.* **47**, 1711 (2001).
 [6] Y. Nagatsu and T. Ueda, *AIChE J.* **49**, 789 (2003).
 [7] Y. Nagatsu and T. Ueda, *Chem. Eng. Sci.* **59**, 3817 (2004).
 [8] J. Chadam, D. Hoff, E. Merino, P. Ortoleva, and A. Sen, *IMA J. Appl. Math.* **36**, 207 (1986).
 [9] C. Wei and P. Ortoleva, *Earth-Sci. Rev.* **29**, 183 (1990).
 [10] A. De Wit and G. M. Homsy, *J. Chem. Phys.* **110**, 8663 (1999).
 [11] Y. Nagatsu, S. K. Bae, Y. Kato, and Y. Tada, *Phys. Rev. E* **77**, 067302 (2008).
 [12] M. Mishra, M. Martin, and A. De Wit, *Phys. Fluids* **19**, 073101 (2007).
 [13] V. Hornof and F. U. Baig, *Exp. Fluids* **18**, 448 (1995).
 [14] H. A. Nasr-El-Din, K. C. Khulbe, V. Hornof, and G. H. Neale, *Rev. Inst. Fr. Pet.* **45**, 231 (1990).
 [15] J. Fernandez and G. M. Homsy, *J. Fluid Mech.* **480**, 267 (2003).
 [16] A. De Wit and G. M. Homsy, *Phys. Fluids* **11**, 949 (1999).
 [17] S. Swernath and S. Pushpavanam, *J. Chem. Phys.* **127**, 204701 (2007).
 [18] S. Swernath and S. Pushpavanam, *Phys. Fluids* **20**, 012101 (2008).
 [19] J. A. Pojman, G. Gunn, C. Patterson, J. Owens, and C. Simmons, *J. Phys. Chem. B* **102**, 3927 (1998).
 [20] J. D'Hernoncourt, A. Zebib, and A. De Wit, *Chaos* **17**, 013109 (2007).
 [21] A. De Wit, P. De Kepper, K. Benyaich, G. Dewel, and P. Borckmans, *Chem. Eng. Sci.* **58**, 4823 (2003).
 [22] Y. Nagatsu, K. Matsuda, Y. Kato, and Y. Tada, *J. Fluid Mech.* **571**, 475 (2007).
 [23] T. Podgorski, M. C. Sostarecz, S. Zorman, and A. Belmonte, *Phys. Rev. E* **76**, 016202 (2007).
 [24] T. Grumstrup and A. Belmonte, *Phys. Fluids* **19**, 091109 (2007).
 [25] L. Gálfi and Z. Rácz, *Phys. Rev. A* **38**, 3151 (1988).
 [26] Z. Jiang and C. Ebner, *Phys. Rev. A* **42**, 7483 (1990).
 [27] S. Cornell, Z. Koza, and M. Droz, *Phys. Rev. E* **52**, 3500 (1995).
 [28] Z. Koza, *J. Stat. Phys.* **85**, 179 (1996).
 [29] A. De Wit, Y. Bertho, and M. Martin, *Phys. Fluids* **17**, 054114 (2005).
 [30] G. Rousseaux, A. De Wit, and M. Martin, *J. Chromatogr., A* **1149**, 254 (2007).
 [31] W. B. Zimmerman and G. M. Homsy, *Phys. Fluids A* **3**, 1859 (1991).